Intrinsic quasi-particle dynamics of topological metallic states

2011 New J. Phys. 13 013008

(http://iopscience.iop.org/1367-2630/13/1/013008)

New Journal of Physics
The open-access journal for physics

Intrinsic quasi-particle dynamics of topological metallic states

S R Park[1,6], W S Jung[1], G R Han[1], Y K Kim[1], Chul Kim[1], D J Song[1], Y Y Koh[1], S Kimura[2], K D Lee[3], N Hur[3], J Y Kim[4], B K Cho[4], J H Kim[5], Y S Kwon[5], J H Han[5] and C Kim[1,7]

[1] Institute of Physics and Applied Physics, Yonsei University, Seoul, Korea
[2] UVSOR Facility, Institute for Molecular Science and The Graduate University for Advanced Studies, Okazaki 444-8585, Japan
[3] Department of Physics, Inha University, Incheon 402-751, Korea
[4] Department of Materials Science and Engineering, GIST, Gwangju 500-712, Korea
[5] Department of Physics, Sungkyunkwan University, Suwon 440-746, Korea
E-mail: changyoung@yonsei.ac.kr

New Journal of Physics **13** (2011) 013008 (11pp)
Received 19 July 2010
Published 11 January 2011
Online at http://www.njp.org/
doi:10.1088/1367-2630/13/1/013008

Abstract. We investigate the intrinsic quasi-particle (QP) dynamics in the topological metallic (TM) states of Bi_2Se_3, $Bi_{2-x}Sn_xTe_3$ ($x = 0.0067$) and Sb. Surprisingly, the intrinsic QP dynamics are mostly determined by the scattering within the TM states and are unaffected by the bulk electronic states. We observe the binding energy-independent imaginary part of the self-energy Im Σ for the QPs in the TM states. We attribute the binding energy-independent Im Σ to momentum mixing due to flakes or warped surfaces of the cleaved samples. This makes the intrinsic scattering rate of the QPs extremely small in the TM states. We discuss a few possible contributions to the smallness of the Im Σ for QPs. Our new observations on the extremely small intrinsic QP scattering rates may open up the possibility of room-temperature quantum devices.

[6] Current address: Department of Physics, University of Colorado, Boulder, CO 80309-0390, USA.
[7] Author to whom any correspondence should be addressed.

Contents

1. Introduction

Topological metallic (TM) states, the metallic surface states of the topological insulator (TI), have attracted much interest among the condensed matter community recently because of their novel properties [1]–[4]. Spin degeneracy, which is normally found in solids, is lifted in TM states. The TM states have odd numbers of Fermi level crossings [2, 4], which results in the protected nature of the TM states. In addition, electron spins in TM are locked into the momenta, forming chiral spin states. Such a spin texture should strongly suppress backscattering by nonmagnetic impurities [5]–[8]. Due to these properties, it is believed that the TM states have high electron mobility and spin-selective current, and they could be used for future spintronic devices [9, 10].

While the chiral spin states have been experimentally measured by spin-resolved photoemission spectroscopy and angle-resolved photoemission spectroscopy (ARPES) [2, 5] and STM [6], the high electron mobility of the TM states is yet to be verified. Even though transport measurement would be the natural method for measuring the mobility, in reality the electrical conductivity is dominated by the bulk contribution [11, 12]. The situation is the same for any other bulk-sensitive technique, such as infrared spectroscopy [11]. We therefore need to use a method that is surface sensitive. In that sense, ARPES is almost a unique tool for measuring the quasi-particle (QP) dynamics of the TM states [13]. For example, the QP dynamics of the TM states in Bi_2Se_3 have been revealed. However, the data showed that the electron scattering in the TM states is almost dominated by the scattering between surface and bulk states [13]. This fact obscures the contribution from the scattering between the TM states, that is, the intrinsic QP dynamics of the TM states.

In a previous report on QP dynamics [13], it was suggested that adsorbates are responsible for scattering between the surface TM states and bulk states. One way to remove such an extrinsic effect is to raise the temperature to get rid of the adsorbates. To obtain information on the intrinsic QP life dynamics of the TM states, we performed temperature-dependent ARPES experiments on various Bi_2Se_3, $Bi_{2-x}Sn_xTe_3$ ($x = 0.0067$) and Sb(111). The newly obtained data do not show any signature of scattering between the TM and bulk states, indicating that the ARPES line shape is mostly determined by the scattering between the TM states. This intrinsic property shows an almost constant scattering rate as a function of binding energy, i.e. extremely low electron–phonon coupling and electron–electron correlation in the TM states.

2. Experimental

Bi_2Se_3 single crystals were grown by the self-flux technique using the published method [14]. $Bi_{2-x}Sn_xTe_3$ ($x = 0.0067$) single crystals were grown by a vacuum Bridgman technique. Sb single crystals were purchased from MaTeck (Germany). ARPES measurements were carried out at the beamline 7U of UVSOR-II [15]. A photon energy of 8 eV was used for Bi_2Se_3 and $Bi_{2-x}Sn_xTe_3$, whereas 10 eV was used for Sb. The total energy resolution was about 5 meV for both photon energies and the angular resolution was about 0.1°. The corresponding momentum resolutions are 0.0016 and 0.002 $Å^{-1}$ for 8 and 10 eV, respectively. The high momentum resolution obtained by using a low photon energy is important in investigating the QP dynamics of the TM states because of the high Fermi velocity of about 3 eV Å. By converting the momentum width to the energy width by multiplying it by the Fermi velocity, a small momentum resolution is amplified by a large Fermi velocity, resulting in a poor energy resolution. In addition, 8 eV photon energy for Bi_2Se_3 and $Bi_{2-x}Sn_xTe_3$ turned out to be crucial in investigating the TM states separately, as the bulk state intensity is relatively weak at these photon energies [13]. Samples were cleaved *in situ* and the chamber pressure was about 1×10^{-10} torr. The experimental temperatures are indicated in the figures.

3. Results

Figures 1(a) and (b) show ARPES data from Bi_2Se_3 near the Fermi level along the Γ–M direction at 12 and 210 K, respectively. Strongly dispersing TM states and broad bulk conduction states are clearly seen at both temperatures. The Fermi cutoff for the high-temperature data is broad due to the thermal broadening effect. Another aspect of the data to note is that there is an upward shift in the band structure as clearly seen by the shift of the time reversal invariant (TRI) point (or Dirac point) at the high temperature (from 0.32 to 0.29 eV). We note that the band shift here should not originate from the band bending due to surface lattice relaxation [5] since the 12 K data taken were from a fresher surface than the high-temperature data. Instead, an upward shift of the band with increasing temperature should be evidence for desorbing adsorbates at high temperatures [13, 17]. It was previously shown that the bulk conduction band bottom is about 0.22 eV higher than the TRI position. This allows us to deduce the bulk band bottom positions at 0.1 and 0.07 eV for 12 and 210 K data, respectively. Figure 1(d) shows the Fermi surface map of Bi_2Se_3 TM states. The Fermi surface is schematically indicated by the red dashed circle and occupies a small portion of the Brillouin zone. The weak photoemission intensity inside the Fermi surface is from the bulk conduction band bottom.

QP dynamics of the TM states can be extracted from the self-energy analysis of the spectral function $A(k,\omega)$, i.e. the ARPES data. $A(k,\omega)$ is proportional to the imaginary part of the single particle Green's function $G(k,\omega)$ and is expressed as

$$A(k,\omega) \propto \mathrm{Im}\, G(k,\omega) = \frac{\mathrm{Im}\, \Sigma(k,\omega)}{(\omega - \varepsilon_k - \mathrm{Re}\, \Sigma(k,\omega))^2 + \mathrm{Im}\, \Sigma(k,\omega)^2},$$

where ε_k, $\mathrm{Re}\,\Sigma$ and $\mathrm{Im}\,\Sigma$ are the bare electron energy and the real and imaginary parts of the self-energy, respectively. $\mathrm{Im}\,\Sigma$ is usually extracted by the half-width at half-maximum (HWHM) of momentum distribution curves (MDC) multiplied by the band velocity [16].

We used the method to extract $\mathrm{Im}\,\Sigma$ from the spectral functions in figures 1(a) and (b) and plot the result in figure 1(c). $\mathrm{Im}\,\Sigma$ from the low-temperature data (blue line) is very similar

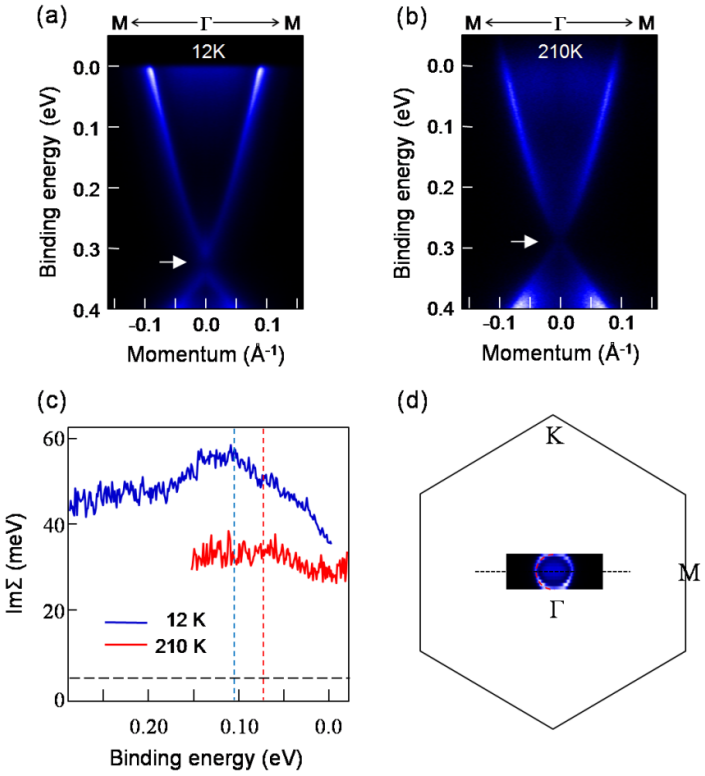

Figure 1. ARPES data from Bi_2Se_3 taken at (a) 12 K and (b) 210 K along the Γ–M direction. The arrows indicate the TRI points. (c) Corresponding Im Σ. The horizontal dashed line indicates the experimental energy resolution. (d) Fermi surface map of Bi_2Se_3.

to the previously reported data [13] and has a 'kink' at about 0.11 eV, as indicated by the blue dashed line. The high temperature data also have a kink at about 0.07 eV. We note that these kink positions coincide with the deduced bulk band bottom positions. This observation confirms that QP dynamics in Bi_2Se_3 TM states is governed by scattering between the TM and bulk states due to impurities or defects [13]. It should also be noted that Im Σ from the high-temperature data (red line) is about 30% smaller than that from low-temperature data. This would be unexpected, considering the fact that a broader line shape is expected in ordinary cases at higher temperatures due to increased electron–phonon coupling or Fermi liquid behavior. However, it is not unexpected because adsorbates that are sources of the scattering between the TM and bulk states can be removed at an elevated temperature. This is also consistent with the upward shift of the band structure as mentioned above. The fact that a smaller kink Im Σ remains in 210 K data indicates that we could not completely remove the adsorbates. These facts suggest that the intrinsic Im Σ of the TM states should be smaller than the values (≈30 meV) in figure 1(c). In addition, there is no appreciable kink structure in the band dispersion or the real part of the self-energy Re Σ, meaning that electron–phonon coupling is very small. These observations (small Im Σ and no kink in Re Σ) reveal that the intrinsic scattering rate for the QPs in the TM states is very small.

It is seen from the Bi_2Se_3 data that Im Σ values of TM of the near E_F TM states are greatly affected by the bulk states. A way to get rid of the bulk state effect is to deprive the

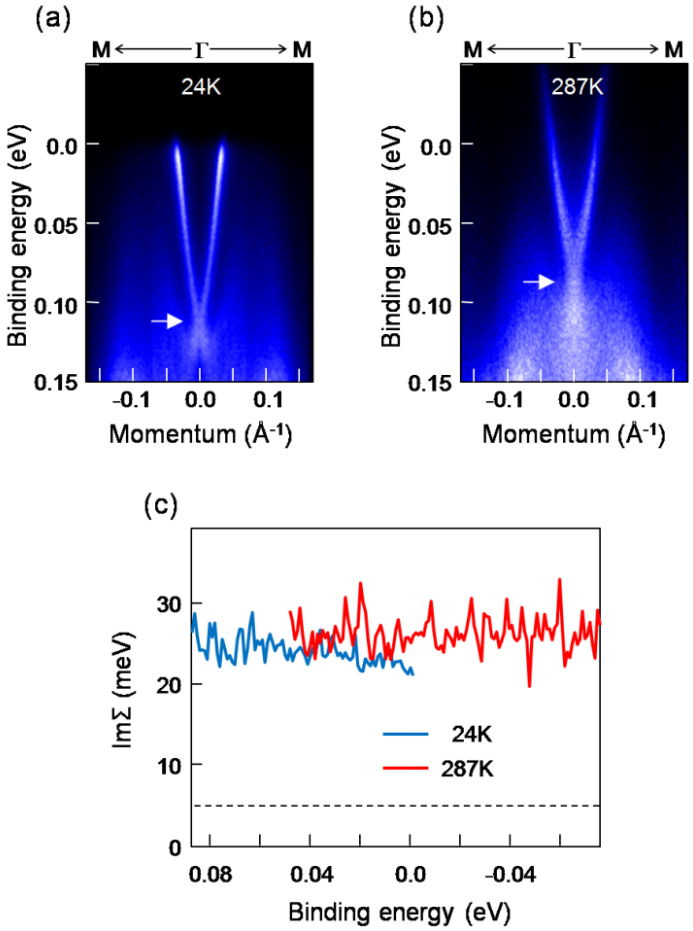

Figure 2. ARPES data from $Bi_{2-x}Sn_xTe_3$ ($x = 0.0067$) taken at (a) 24 K and (b) 287 K along the Γ–M direction. (c) Corresponding Im Σ. The horizontal dashed line indicates the experimental resolution. The shift of the TRI point is attributed to the photovoltaic effect.

bulk of near E_F states. It was shown that the Fermi level lies within the gap for $Bi_{2-x}Sn_xTe_3$ ($x = 0.0067$) [17]. Figures 2(a) and (b) show ARPES data from $Bi_{2-x}Sn_xTe_3$ ($x = 0.0067$) near the Fermi level along the Γ–M direction at 24 and 287 K, respectively. The sharp and strongly dispersive band is the TM band, and the weak and broad features outside the TM band are from the bulk valence bands. We note that the TRI point (white arrow) is located about 0.15 eV below the bulk valence band maximum [17]. This contrasts with the Bi_2Se_3 case for which the bulk valence band maximum exists below the TRI point. The TRI point of $Bi_{2-x}Sn_xTe_3$ ($x = 0.0067$) grown by the Bridgman method has a binding energy of about 0.11 eV, which corresponds to the TRI position for $x = 0.009$ samples grown by the self-flux method [17]. Comparing the low- and high-temperature data, it is clearly seen that the high-temperature data have a very broad Fermi edge due to the thermal broadening, making the ARPES spectral function dispersal more than 50 meV above the Fermi level. We also note that the TRI point is shifted to a lower binding energy. This shift is not due to doping from the adsorbates (otherwise, we would have observed the bulk state effect) but to the photovoltaic effect [18].

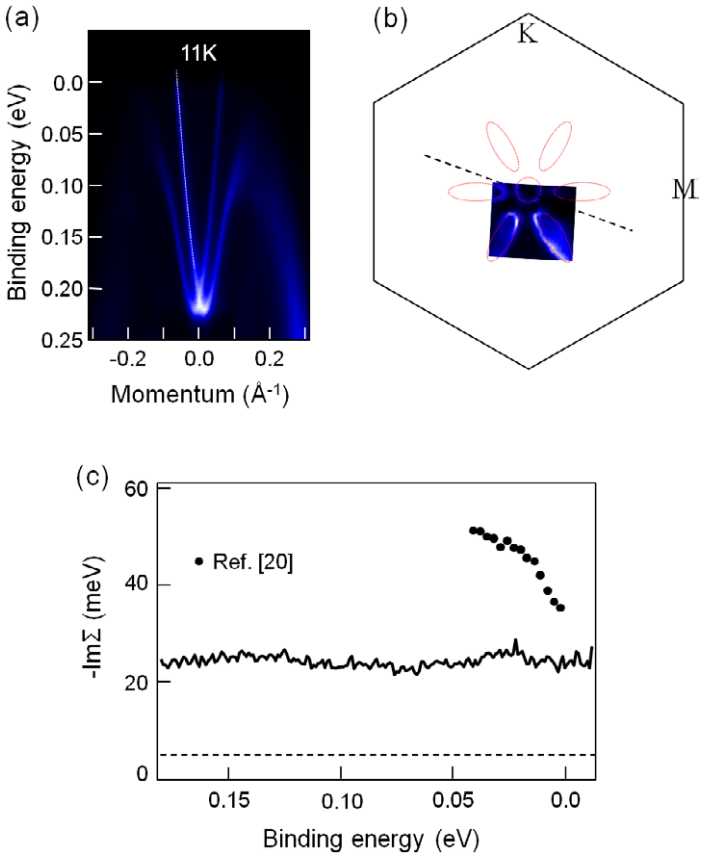

Figure 3. (a) ARPES data from Sb(111) taken at 11 K along the dashed line in (b). White dotted line marks the MDC peak positions. (b) Fermi surface plot of Sb(111). (c) Im Σ extracted from the data in (a) and the previously reported data of Sugawara *et al* [20]. The horizontal dotted line indicates the experimental resolution.

We pay attention to the QP dynamics or Im Σ in figure 2(c), which are extracted from the data in figures 2(a) and (b). Im Σ is almost constant and remains independent of the binding energy and temperature. This is in strong contrast with the Bi_2Se_3 case, in which the bulk density of states (DOS) effect was very clear. Therefore, the absence of energy-dependent features, especially the kink in Im Σ means that the scattering of a QP in the TM band to a bulk state has been shut off. It is not very clear at this moment what causes the difference and a discussion of this will be given in the next section. Whatever the reason, it is clear that the total line width is about 25 meV and that Im Σ is binding energy independent. Note that the total width contains both intrinsic and extrinsic effects. Considering that the binding energy-independent width usually means extrinsic effects such as momentum mixing, it is clear that the intrinsic line width of the TM states is smaller than 25 meV. In addition, as is the case for Bi_2Se_3, no appreciable kinks in the dispersion are observed. Such a small Im Σ value and the absence of kinks in the dispersion are similar to the Bi_2Se_3 case and show that the intrinsic QP scattering rate is small in $Bi_{2-x}Sn_xTe_3$.

Even though not an insulator, Sb has relevance, as will be discussed below. Figure 3(a) plots ARPES data from Sb(111) surface states along the dashed line on the Fermi surface map

in figure 3(b). Sb(111) surface states split due to the Rashba effect and an odd number of bands cross the Fermi level along the Γ–M direction as shown in the figure. Therefore, the surface states of Sb(111) are nontrivial although the bulk is a metal [6, 19]. We extract Im Σ from data in figure 3(a) using the same method and plot the extracted Im Σ in figure 3(c). Our data are more than twice as sharp as the previously reported one by Sugawara *et al* [20] as compared in figure 3(c). It is probably because of the high momentum resolution in our low-photon-energy ARPES which gives us an opportunity to discuss the intrinsic line shape of the Sb(111) TM states. Remarkably, the Im Σ of Sb(111) TM states remains almost constant down to 0.18 eV. Band dispersion in figure 3(a) also shows no kink structure. These observations show that a very small QP scattering rate is intrinsic and is a common feature of the TM states for Bi_2Se_3, $Bi_{2-x}Sn_xTe_3$ and Sb.

4. Discussion

Experimental results from Bi_2Se_3, $Bi_{2-x}Sn_xTe_3$ and Sb *directly* show that Im Σ of QPs in TM states is very small. Moreover, Im Σ is binding energy independent for $Bi_{2-x}Sn_xTe_3$ and Sb. In fact, there is some indication that this is also the case for Bi_2Se_3, because Im Σ became smaller and flatter (less kink in Im Σ) as the temperature was raised to 210 K. Had the adsorbates on the surface been completely removed, Im Σ would have been binding energy independent for Bi_2Se_3. This observation suggests that the measured line width for the TM states should be more or less binding energy independent. Such a binding energy independent Im Σ usually indicates that most of the Im Σ actually has extrinsic origin, as we argued above.

To discuss the origin of Im Σ, we need to discuss the scattering channels in $Bi_{2-x}Sn_xTe_3$ ($x = 0.0067$) and Sb to find the influence of the bulk DOS. The Bi_2Se_3 case has already been discussed in our previous report [13]. In these materials, scattering between the TM and bulk states is also expected to be strong, but the situations are different from that of Bi_2Se_3 because the bulk DOS are different. For $Bi_{2-x}Sn_xTe_3$ ($x = 0.0067$), the Fermi level lies near the top of the valence band, as schematically shown in figure 4(a) [17]. On the other hand, Sb is a metal and therefore has no gap as depicted in figure 4(c) [20]. With the given bulk DOS, a QP (photo-hole) in the TM band can be scattered into a bulk state due to electron–electron interaction, electron–phonon coupling and impurity-created disorder potential.

A rough estimate of the Im Σ (or $1/\tau$) for $Bi_{2-x}Sn_xTe_3$ and Sb can be obtained by calculating the available phase space volume. Results at 0 K are schematically shown in figures 4(b) and (d). Im Σ for $Bi_{2-x}Sn_xTe_3$ is zero up to E_g since a minimum energy of E_g is required to create electron–hole (e–h) pair creation processes (electron–electron interaction). It then increases in proportion to the binding energy square. Electron–phonon coupling, on the other hand, gives an Im Σ that is initially zero up to the phonon energy ω_0 and then proportional to the bulk DOS. Finally, Im Σ from the impurity-created disorder potential is proportional to the bulk DOS because this channel involves elastic scatterings. For Sb, the bulk is a metal and thus does not have a band gap. In that case, the Im Σ of $Bi_{2-x}Sn_xTe_3$ can be shifted upward by E_g for Im Σ from the e–h pair. For electron–phonon coupling and impurity scattering, the situation is very similar to the $Bi_{2-x}Sn_xTe_3$ case.

The above results show that none of the channels give binding-independent Im Σ. The situation is similar even if we consider the scattering channels between the TM states as the surface state DOS should be linear in binding energy. Binding energy independence is usually a strong indication of the extrinsic effect. We therefore attribute the constant term in Im Σ to an

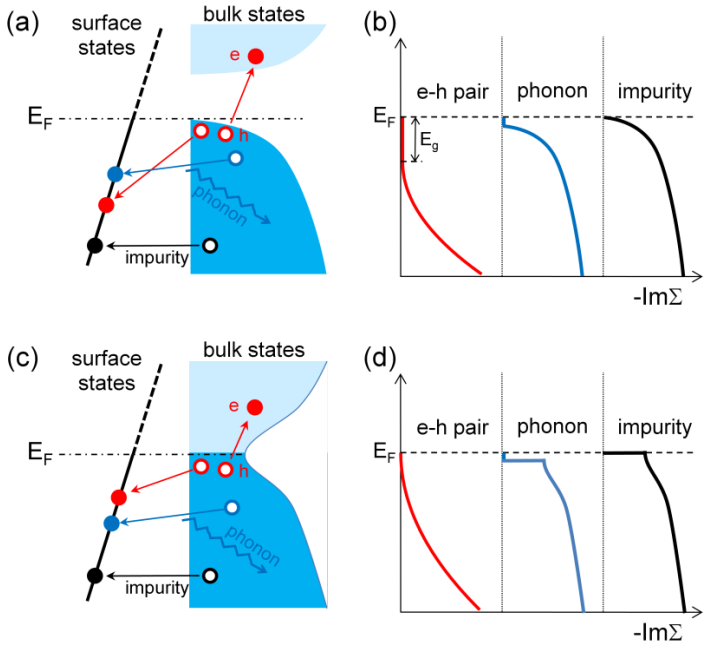

Figure 4. (a) Illustration of various scattering channels for a photo-hole in the TM band to the bulk states for the $Bi_{2-x}Sn_xTe_3$ case. Only the transitions to the bulk states are considered. (b) Schematics of the imaginary part of the self-energies Im Σ for various channels. (c) Various scattering channels for a photo-hole in the TM band to metallic bulk states for Sb. (d) Corresponding Im Σ for the various channels illustrated in (c).

extrinsic origin, such as the momentum mixing from uneven surfaces (flakes and warping) of the samples. To summarize, our new experimental results show that (i) scattering channels from TM to bulk states are shut off and thus QPs in the TM states either do not scatter or scatter very little into the bulk states (otherwise we would see an Im Σ bearing the shape of the bulk DOS) and (ii) a major part of Im Σ comes from the extrinsic effect, making intrinsic Im Σ much smaller than the observed total width of 25 meV. We stress that these conclusions are robust independent of the following discussions.

Having found that Im Σ is very small for the TM states, we want to compare Im Σ values of Bi_2Se_3, $Bi_{2-x}Sn_xTe_3$ and Sb with those from other materials. We plot the extracted Im Σ from the ARPES spectral functions of $Bi_{2-x}Sn_xTe_3$, Sb, graphene [21] and $Bi_2Sr_2CaCu_2O_{8-\delta}$ (Bi2212) nodal direction [22] and the large hole pocket near the Γ of LiFeAs [23] in figure 5. We see that Im Σ values of Bi2212 and LiFeAs drastically increase with binding energy due to electron–phonon interaction [24, 25] and electron–electron interaction [26] and have more than 50 meV of Im Σ at 0.1 eV binding energy. However, Im Σ of TM has no binding energy dependence and shows a small QP scattering rate from 0 to 180 meV binding energy. Once we subtract the constant term, we are left with a very small value of Im Σ for $Bi_{2-x}Sn_xTe_3$ and Sb. Our experimental observation reveals that electron–phonon coupling and electron–electron correlation in the TM states are, if any, much smaller than those found in Bi2212 or LiFeAs. As mentioned above, the band dispersions do not show any discernable kink structures either, which is consistent with extremely small electron–phonon coupling. In addition, the fact that the

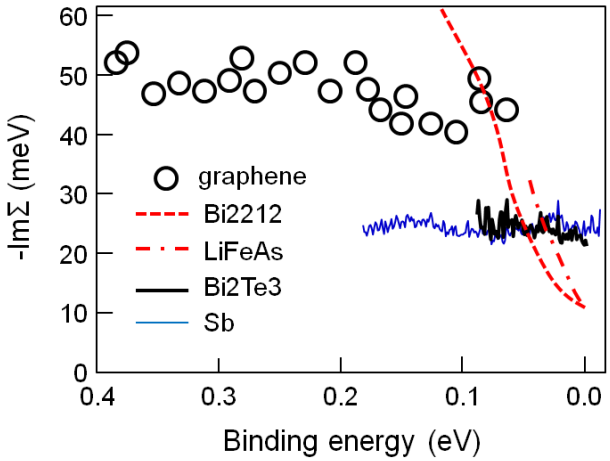

Figure 5. Plot of ImΣ from $Bi_{2-x}Sn_xTe_3$, Sb, graphene [20], Bi2212 [22] and LiFeAs [23].

measured and calculated bandwidths are very similar also confirms that the electron–electron interaction is fairly small [3].

It is also interesting to compare the data with that of graphene. The QP scattering rate of the TM states is even smaller than that of graphene, as shown in figure 5 [21]. The mobility of graphene is known to be very high, even showing a room-temperature quantum Hall effect [27]. As our results show very small QP scattering rates, the QPs must have a very long lifetime (and thus high mobility) even at room temperature. How do graphene and TM compare? DOS at the Fermi level is comparable for graphene and $Bi_{2-x}Sn_xTe_3$, and both have chiral spins (pseudo-spin for graphene). These should make scattering rates comparable for the QPs in graphene and TMs. However, the relevant orbitals in TIs ($6p$ for $Bi_{2-x}Sn_xTe_3$ and $5p$ for Sb) are larger than that of graphene ($2p$). Contrary to the uniform local DOS (LDOS) of the TM states, graphene LDOS is strongly localized near the carbon atom [28]. This causes significant electron–phonon coupling in the states [29]. In this sense, we expect that QP scattering rates in the TM states are much smaller than that of graphene. If that is the case, this may open up a possibility of room-temperature quantum oscillation in the TM states. Experimental observation of such a phenomenon will be an important step toward the implementation of TIs in quantum computing [30].

Then, a natural question arises as to why electron–electron correlation and electron–phonon coupling are extremely small in the TM states. We believe that multiple mechanisms factor into the observed small interactions. First of all, the small Fermi surface volume for the TM states (figures 1(d) and 3(b)) makes the available phase space very small for electron–phonon coupling and e–h pair creation. For example, the DOS of $Bi_{2-x}Sn_xTe_3$ and Sb at Fermi energy is roughly $1/40$ and $1/4$ of that of Bi2212, respectively, making the interactions that much smaller. Secondly, spin chirality of the TM states is also partly responsible because it reduces the available phase space for an electron to scatter to. It especially suppresses the back scattering. This factor is well understood and has been discussed in recent STM work on TIs [6]–[8]. Finally, the relatively large orbital size of the TM states (6p for $Bi_{2-x}Sn_xTe_3$ and 5p for Sb) tends to reduce not only electron–electron correlation but also electron–phonon coupling. A large overlap between the orbitals makes the charge distribution uniform, making

the electron–phonon coupling and electron–electron correlation small. Indeed, LDOS of the TM states measured by STM is uniform, indicating that the wave function is well spread [31].

The last question that remains to be answered is: Why are the TM and bulk states decoupled in clean samples? Our results for binding energy-independent QP scattering rates indicate that QPs hardly scatter into bulk states in high-quality samples with clean surfaces. This is rather unexpected because geometrically there should be a finite overlap between the TM and bulk states. The narrow scattering region due to the short penetration depth of a TM state into bulk [32] and good screening by high-mobility TM electrons may significantly reduce the scattering between the TM and bulk states, but it is unclear whether those are enough to explain such a suppression of the scattering between the TM and bulk states. Further studies are needed to clarify this issue.

Acknowledgments

This work was supported by the NRF (contract no. 20090080739) and the KICOS under grant no. K20602000008. This work was performed as part of a joint studies program of the Institute for Molecular Science in 2009. NH acknowledges support from the Korea Research Foundation through KRF-2008-331-C00093.

References

[1] Fu L, Kane C L and Mele E J 2007 *Phys. Rev. Lett.* **98** 106803
[2] Hsieh D, Qian D, Wray L, Xia Y, Hor Y S, Cava R J and Hasan M Z 2008 *Nature* **453** 970
[3] Zhang H, Liu C X, Qi X L, Dai X, Fang Z and Zhang S C 2009 *Nat. Phys.* **5** 438
[4] Xia Y *et al* 2009 *Nat. Phys.* **5** 398
[5] Hsieh D *et al* 2009 *Nature* **460** 1101
[6] Roushan P, Seo J, Parker C V, Hor Y S, Hsieh D, Qian D, Richardella A, Hasan M Z, Cava R J and Yazdani A 2009 *Nature* **460** 1106
[7] Zhang T *et al* 2009 *Phys. Rev. Lett.* **103** 266803
[8] Alpichshev Z, Analytis J G, Chu J H, Fisher I R, Chen Y L, Shen Z X, Fang A and Kapitulnik A 2010 *Phys. Rev. Lett.* **104** 016401
[9] Day C 2008 *Phys. Today* **61** 19
[10] Moore J 2009 *Nature* **460** 1090
[11] Butch N P, Kirshenbaum K, Syers P, Sushkov A B, Jenkins G S, Drew H D and Paglione J 2010 *Phys. Rev.* B **81** 241301
[12] Hor Y S *et al* 2010 *Phys. Rev.* B **81** 195203
[13] Park S R, Jung W S, Kim Chul, Song D J, Kim C, Kimura S, Lee K D and Hur N 2010 *Phys. Rev.* B **81** 041405
[14] Hor Y S, Richardells A, Poushan P, Xia Y, Checkelsky J G, Yazdani A, Hazsan M Z, Ong N P and Cava R J 2009 *Phys. Rev.* B **79** 195208
[15] Kimura S *et al* 2010 *Rev. Sci. Instrum.* **81** 053104
[16] Bogdanov P V *et al* 2000 *Phys. Rev. Lett.* **85** 2581
[17] Chen Y L *et al* 2009 *Science* **325** 178
[18] Kordyuk A A *et al* 2010 arXiv:1009.4855v1
[19] Gomes K K, Ko W, Mar W, Chen Y, Shen Z X and Manoharan H C 2010 arXiv:0909.0921
[20] Sugawara K, Sato T, Souma S, Takahashi T, Arai M and Sasaki T 2006 *Phys. Rev. Lett.* **96** 046411
[21] Sprinkle M *et al* 2009 *Phys. Rev. Lett.* **103** 226803
[22] Koralek J D *et al* 2006 *Phys. Rev. Lett.* **96** 017005

[23] Kim Y K and Kim C 2010 private communication
[24] Lanzara A *et al* 2001 *Nature* **412** 510
[25] Koitzsch A *et al* 2009 *Phys. Rev. Lett.* **102** 167001
[26] Casey P A *et al* 2008 *Nat. Phys.* **4** 210
[27] Novoselov K S, Jiang Z, Zhang Y, Morozov S V, Stormer H L, Zeitler U, Maan J C, Boebinger G S, Kim P and Geim A K 2007 *Science* **315** 1379
[28] Rutter G M *et al* 2007 *Science* **317** 219
[29] Yan Y *et al* 2007 *Phys. Rev. Lett.* **98** 166802
[30] Akhmerov A R, Nilsson J and Beenakker C W J 2009 *Phys. Rev. Lett.* **102** 216404
[31] Hanaguri T *et al* 2010 *Phys. Rev.* B **82** 081305
[32] Zhang W, Yu R, Zhang H J, Dai X and Fang Z 2010 *New J. Phys.* **12** 065013